

# Estimates of the Ground Accelerations at Point Reyes Station during the 1906 San Francisco Earthquake

by Abdolrasool Anooshehpour, Thomas H. Heaton, Baoping Shi, and James N. Brune

**Abstract** We have developed an analytical solution for the rocking and overturning response of a two-dimensional, symmetric rigid block subject to a full sine wave of horizontal ground acceleration. We use this solution to provide lower-bound estimates of the peak ground acceleration at Point Reyes Station, California, during the 1906 San Francisco earthquake that toppled the San Francisco-bound train. Our results, for a 3% damping ratio, indicate that for a single cycle of a sine wave the minimum toppling accelerations at 1, 1.5, and 2 Hz are 0.35g, 0.5g, and 1.05g, respectively. For more realistic accelerograms the toppling accelerations are about 1.1g (complex synthetic) and 0.76g (Lucerne record of the 1992 Landers earthquake).

## Introduction

It has long been recognized that most of the slip along plate boundaries occurs during the largest-magnitude earthquakes. Although the frequency of earthquakes decreases by about a factor of 10 with each unit of magnitude, the seismic moment increases by a factor of 32. Thus, great earthquakes on the San Andreas fault, while infrequent, are inevitable: these great earthquakes are the main actors in California plate tectonics. So while the average repeat interval of these great earthquakes may be hundreds of years, it is clear that future urbanized areas of California will be subjected to these earthquakes.

What is it like to be close to a great earthquake on the San Andreas fault? Unfortunately, there are no ground motion recordings of any great shallow crustal earthquakes. Hall and others (1995) discuss the nature of near-source ground motions from large crustal earthquakes, and they emphasize the importance of large-amplitude displacement pulses that occur in the near-source region. In particular, when rupture is propagating toward a site located near a fault, the pulses are largest in the direction perpendicular to the rupture surface, and they have displacement amplitudes that are roughly comparable to the fault slip. Haskell (1969) argued persuasively that such pulses should exist, and he suggested that they can be seen in ground motions recorded during the 1966 Parkfield earthquake. Numerous other examples of these pulses have been recorded in recent moderate-sized earthquakes, and some of these examples are shown in a report by Hall et al. (1995, Fig. 2 therein). While the existence of near-source displacement pulses is now well accepted, the nature of such pulses in great earthquakes is still a subject of discussion. In particular, the near-source displacement amplitudes recorded in the 1994 Northridge and 1995 Kobe earthquakes did not exceed 70 cm (Hall *et*

*al.*, 1995). However, much larger displacements are expected in great earthquakes that have larger fault slips.

Perhaps the best example of ground motion recorded close to a fault with large slip is the Lucerne accelerogram, which was recorded on rock about 1 km from the trace of the 1992 Landers earthquake. Iwan and Chen (1994) processed these accelerograms, giving particular consideration to accurately recovering ground displacement in an inertial coordinate frame. Their processed displacement is dominated by a 4-sec pulse of displacement having a maximum amplitude of 255 cm. Wald and Heaton (1994) demonstrated that the observed displacement pulse can be reproduced by a fault-slip model that is compatible with other data including strong ground motions, teleseismic body waves, geodetic deformations, and surface fault offsets. Hartzell and Heaton (1995) and Archuleta and Seale (1995) both produced long-period ground motions with striking similarities to the Lucerne record in a 1990 workshop to predict the motions from a hypothesized  $M$  7.5 strike-slip earthquake (the displacement records from the Hartzell and Heaton (1995) simulation are also reproduced in the paper by Hall *et al.* [1995]).

A remarkable account of a long-period displacement pulse that overturned a train at Point Reyes Station during the 18 April 1906 San Francisco earthquake ( $M$  7.8) is described by Jordan (1907). The overturned train is shown in Figure 1, and a sketch map showing the location of the train and the San Andreas fault are shown in Figure 2. The train was pointing southeastward approximately parallel to the fault when the earthquake struck. The following passage is from Jordan's description (p. 19).

At Point Reyes Station at the head of Tomales Bay the 5:15 train for San Francisco was just ready. The con-



Figure 1. The San Francisco-bound train at Point Reyes Station that was tipped on its side during the 1906 San Francisco earthquake.

ductor had just swung himself on when the train gave a great lurch to the east (from which we infer that the ground initially moved southwest), followed by another to the west (from which we infer that the ground then moved back to the northeast), which threw the whole train on its side. The astonished conductor dropped off as it went over, and at the sight of the falling chimneys and breaking windows of the station, he understood that it was the Temblor. The fireman turned to jump from the engine to the west when the return shock came. He then leaped to the east and borrowing a Kodak he took the picture of the train here presented.

In this paper, we present an analysis of the characteristics of ground motion pulses that are consistent with the story of the tipped train at Point Reyes station. The account given above suggests a pulse of displacement in the southwest direction. This is consistent with the polarization expected for an *SH* wave propagating to the northwest produced by rupture on the San Andreas fault that is approaching Point Reyes Station from the southeast. If the rupture was approaching from the northwest, then we would expect a displacement pulse in the northeast direction. Thus

the current observation seems consistent with the epicenter located approximately 40 km to the southeast near the Golden Gate, as inferred by Bolt (1968). We begin by developing an analytical solution for the rocking and overturning of a two-dimensional rigid block subject to a full sine wave of horizontal ground acceleration. The solution, when applied to the toppled train, provides a lower-bound estimate of the peak ground acceleration at Point Reyes Station. (We assume a full sine-wave shape for the fault-normal acceleration pulse.) The analysis is extended to more realistic situations using a synthetic accelerogram generated for a magnitude 8 earthquake, and the Lucerne record of the 1992 Landers earthquake.

### Analytical Solution

Following Housner (1963), Shi *et al.* (1996) developed an analytical solution for the rocking response of a two-dimensional, symmetric rigid block (Fig. 3) subject to a half sine wave of ground acceleration. Here, we consider the rocking response of a rigid block subject to a full sine wave of horizontal ground acceleration that is defined as

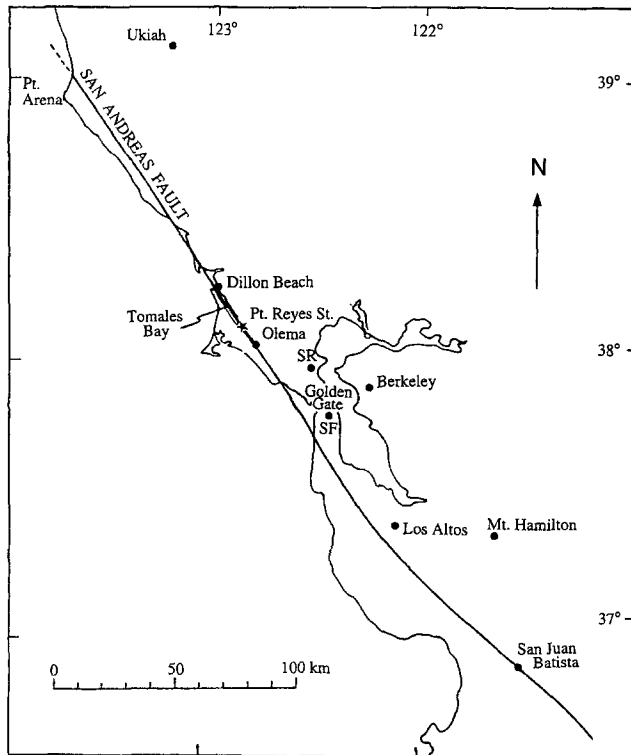


Figure 2. A map showing the San Andreas fault and Point Reyes Station (from Boore, 1977).

$$a(t) = \begin{cases} -A \sin(\omega t + \psi) & -\frac{\psi}{\omega} \leq t \leq \frac{2\pi - \psi}{\omega} \\ 0 & \text{otherwise} \end{cases}, \quad (1)$$

where  $\omega$  is the angular frequency,  $A$  is the acceleration amplitude, and  $\psi$  is defined by

$$\psi = \sin^{-1} \left( \frac{\alpha g}{A} \right). \quad (2)$$

to ensure that at time  $t = 0$  the inertial force due to ground acceleration is large enough to overcome the restoring force ( $\alpha g$ ) and to initiate the rocking motion.

Referring to Figure 3, the overturning problem we are interested in can be described as follows. Initially, at  $t = 0$  when ground acceleration exceeds  $\alpha g$ , the block starts rocking clockwise about  $O_1$ ; then, after rotating through an angle  $\theta$ , it comes to rest; at this point, the block changes direction and rotates counterclockwise until its impact with the base. At the time of impact ( $t = t_i$ ),  $O_2$  comes in contact with the base, while  $O_1$  loses contact. After impact, the block continues to rotate counterclockwise about  $O_2$ . Its angular velocity decreases gradually until it becomes *nearly* zero just when the angular displacement exceeds  $\alpha$ ; at this point, because of its weight, the block overturns. It is assumed that the coefficient of friction is sufficiently large so that there will

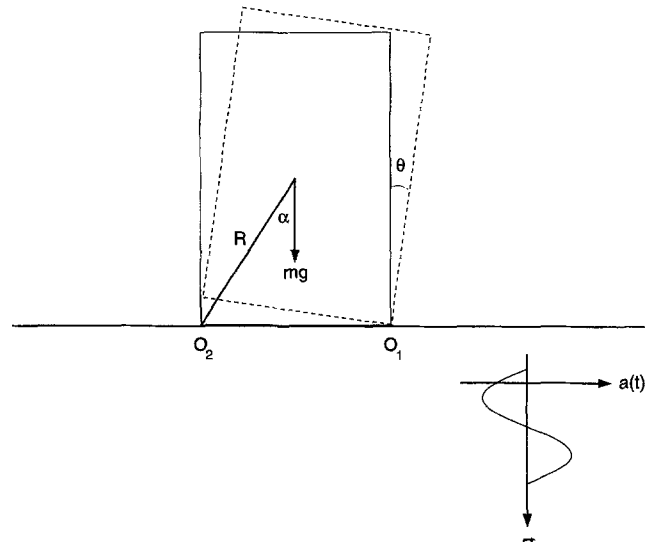


Figure 3. Rocking of a rigid block subject to a full sine wave of ground acceleration,  $a(t)$ .

be no sliding between the block and the base (Housner, 1963).

#### Equation of Motion

For a symmetric rigid block subject to ground accelerations  $a$ , the differential equation of motion about an axis of rotation is

$$I\ddot{\theta} = -mgR \sin(\alpha - \theta) + mRa \cos(\alpha - \theta), \quad (3)$$

where  $g$  is the acceleration due to gravity,  $m$  is the mass of the block,  $R$  is the distance between the center of mass to the rocking axis,  $I$  is the moment of inertia about the rocking axis;  $\theta$  is the instantaneous angular displacement of the block, and  $\alpha$  is the maximum angular displacement of the block from its equilibrium position without being overturned. Assuming that  $\alpha$  is small ( $<15^\circ$ ), the equation of motion reduces to

$$\ddot{\theta} - p^2(\theta - \alpha) = \frac{mRa}{I} \quad (4)$$

where

$$p = \sqrt{\frac{mgR}{I}}.$$

#### Overturning by Sinusoidal Acceleration

The overturning of a rigid block (Fig. 3) by the full sine wave of ground acceleration specified by equation (1) involves an impact. During the course of rocking, depending on the frequency of the ground acceleration,  $\omega$ , impact can occur either before or after the instant that the ground acceleration has completed its full cycle, namely, at

$\tau = 2\pi - \psi/\omega$ . Hence we consider two cases: (1)  $t_i < \tau$ , and (2)  $t_i > \tau$ .

CASE 1:  $t_i < \tau$ . For low-frequency ground accelerations for which the impact occurs at  $t < \tau$ , we divide the interval from the time that the rocking motion begins ( $t = 0$ ) to the time that the block overturns ( $t > \tau$ ) into three time windows: (a)  $0 \leq t \leq t_i$ , (b)  $t_i < t \leq \tau$ , and (c)  $t > \tau$  and solve the corresponding differential equations.

(a) By substituting for  $a$  in equation (4), the differential equation of motion for the interval  $0 \leq t \leq t_i$  becomes

$$\ddot{\theta}_1 - p^2\theta_1 = p^2\alpha \left[ \frac{\sin(\omega t + \psi)}{\sin \psi} - 1 \right]. \quad (5)$$

This equation, subject to the conditions  $\theta_1 = 0$  and  $\dot{\theta}_1 = 0$  at  $t = 0$ , has the solution

$$\theta_1 = \alpha + \frac{\alpha}{1 + \left(\frac{\omega}{p}\right)^2} \left[ -\left(\frac{\omega}{p}\right)^2 \cosh pt + \frac{\omega \sinh pt}{p \tan \psi} - \frac{\sin(\omega t + \psi)}{\sin \psi} \right]. \quad (6)$$

(b) After impact,  $t > t_i$ , the role of the inertial force on the rocking of the block reverses; that is, if just before the impact the ground acceleration were to enhance the effective restoring force, immediately after the impact it would reduce it, or vice versa. Therefore, the differential equation of motion for the time interval  $t_i < t \leq \tau$  becomes

$$\ddot{\theta}_2 - p^2\theta_2 = p^2\alpha \left[ -\frac{\sin(\omega t + \psi)}{\sin \psi} - 1 \right]. \quad (7)$$

The solution to equation (7), subject to the following initial conditions at  $t = t_i$ ,

$$\begin{aligned} \theta_2(t_i^+) &= \eta\theta_1(t_i^-) \\ \dot{\theta}_2(t_i^+) &= -\eta\dot{\theta}_1(t_i^-) \end{aligned}$$

is

$$\begin{aligned} \theta_2 = & \alpha - \alpha(1 - \eta) \cosh p(t - t_i) \\ & - \frac{\alpha}{1 + \left(\frac{\omega}{p}\right)^2} \left[ \eta\left(\frac{\omega}{p}\right)^2 \cosh p(t - 2t_i) \right. \\ & + \eta \frac{\omega \sinh p(t - 2t_i)}{p \tan \psi} + (1 + \eta) \frac{\sin(\omega t_i + \psi)}{\sin \omega} \\ & \left. \cosh p(t - t_i) + (1 - \eta) \frac{\omega \cos(\omega t_i + \psi)}{p \sin \psi} \right. \\ & \left. \sinh p(t - t_i) - \frac{\sin(\omega t + \psi)}{\sin \psi} \right], \quad (8) \end{aligned}$$

where  $\eta$ , the coefficient of restitution, indicates a reduction in the rocking energy of the block as a result of its impact with the base. Assuming that there is no bouncing at the time of impact (Housner, 1963), the angular momentum about  $O_2$  immediately before impact is equal to that immediately after impact (there is no external torque because the impact force is assumed to act at  $O_2$ ); that is,

$$I\dot{\theta}_1(t_i^-) - 2mR^2 \sin^2 \alpha \dot{\theta}_1(t_i^-) = I\dot{\theta}_2(t_i^+). \quad (9)$$

Therefore,

$$\begin{aligned} \eta &= \left| \frac{\dot{\theta}_2(t_i^+)}{\dot{\theta}_1(t_i^-)} \right| \\ &= 1 - \frac{2mR^2}{I} \sin^2 \alpha. \quad (10) \end{aligned}$$

For the rectangular block of Figure 3 (assuming that  $\alpha$  is small),  $\eta$  has the simple expression

$$\eta = 1 - \frac{3}{2} \alpha^2.$$

(c) Finally, for  $t \geq \tau$  the equation of motion, in the absence of inertial force, reduces to

$$\ddot{\theta}_3 - p^2(\theta_3 - \alpha) = 0. \quad (11)$$

The solution to this equation subject to initial conditions at  $t = \tau$ :

$$\begin{aligned} \theta_3(\tau^+) &= \theta_2(\tau^-) \\ \dot{\theta}_3(\tau^+) &= \dot{\theta}_2(\tau^-) \end{aligned}$$

is

$$\begin{aligned} \theta_3 = & \alpha - \alpha(1 - \eta) \cosh p(t - t_i) \\ & - \frac{\alpha}{1 + \left(\frac{\omega}{p}\right)^2} \left[ \eta\left(\frac{\omega}{p}\right)^2 \cosh p(t - 2t_i) \right. \\ & + \eta \frac{\omega \sinh p(t - 2t_i)}{p \tan \psi} + (1 + \eta) \frac{\sin(\omega t_i + \psi)}{\sin \psi} \\ & \left. \cosh p(t - t_i) + (1 - \eta) \frac{\omega \cos(\omega t_i + \psi)}{p \sin \psi} \right. \\ & \left. \sinh p(t - t_i) - \frac{\omega \sinh p(t - \tau)}{p \sin \psi} \right]. \quad (12) \end{aligned}$$

Combining equations (6), (8), and (12), we can write the solution for the entire duration as

$$\theta(t) = \theta_1(t)H(t_i - t) + \theta_2(t)H(t - t_i)H(\tau - t) + \theta_3(t)H(t - \tau) \quad (13)$$

where  $H(t)$  is the Heaviside unit step function defined as

$$H(t) = \begin{cases} 0 & t < 0 \\ 1 & t > 0 \end{cases}$$

Figure 4 shows a plot of the normalized angular displacement  $\theta/\alpha$  (equation 13) versus dimensionless time  $t/\tau$  for  $\omega/p = 4$  and  $\eta = 0.95$ . The minimum toppling acceleration amplitude is about  $1.70\alpha g$ ; and the impact occurs at  $t = 0.74\tau$ . The ground acceleration and the angular velocity of the block are also given on the same plot.

**Minimum Overturning Amplitude.** The minimum overturning condition (the minimum ground acceleration amplitude at a given frequency,  $\omega$ , that topples the block) requires that  $\dot{\theta}_3 = 0$  at  $\theta_3 = \alpha$  (i.e., that the block at the time of overturning must have nearly zero angular velocity). Using the conservation of total energy, this condition is satisfied if

$$\frac{1}{2} I \dot{\theta}_3^2(\tau) = mgR [1 - \cos(\alpha - \theta_3(\tau))]. \quad (14)$$

Again, using the small angle approximation,  $\cos(\alpha - \theta_3) \approx 1 - \frac{1}{2}(\alpha - \theta_3)^2$ , equation (14) reduces to

$$\dot{\theta}_3^2(\tau) = \frac{mgR}{I} [\alpha - \theta_3(\tau)]^2,$$

or

$$\dot{\theta}_3(\tau) = p[\alpha - \theta_3(\tau)]. \quad (15)$$

Finally, by substituting for  $\dot{\theta}_3(\tau)$  and  $\theta_3(\tau)$  in equation (15), the minimum overturning condition (maximum  $\psi$ ) is obtained:

$$\tan \psi = \frac{p/\omega}{1 - [1 + (p/\omega)^2] (1 - \eta^{-1})e^{p t_i}} \left[ -1 - (1 + \eta^{-1}) \frac{p}{\omega} \frac{\sin(\omega t_i + \psi)}{\cos \psi} e^{p t_i} + (1 - \eta^{-1}) \frac{\cos(\omega t_i + \psi)}{\cos \psi} e^{p t_i} + \frac{e^{-p(\tau - 2t_i)}}{\eta \cos \psi} \right]. \quad (16)$$

Equation (16) specifies the amplitude  $A (= \alpha g / \sin \psi)$  of the sinusoidal ground acceleration given by equation (1) as a function of  $\omega/p$  that just overturns the block, provided that  $t_i$  is known. However,  $t_i$  is determined from equation (6), subject to the condition that the block is in vertical position

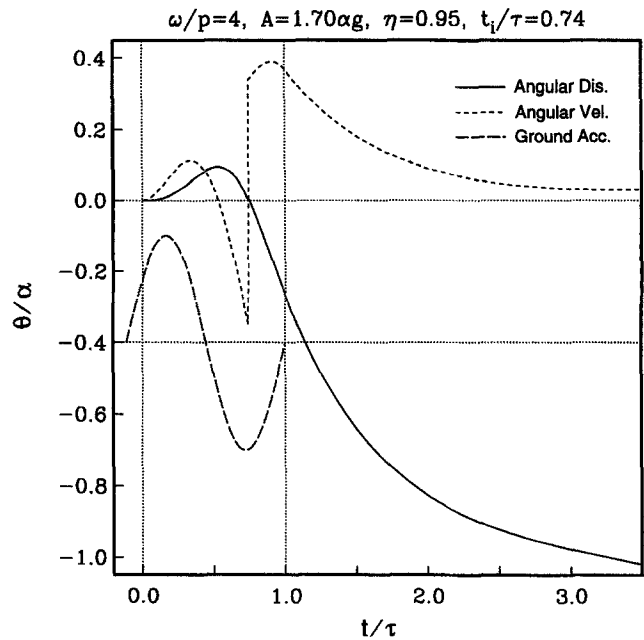


Figure 4. A plot of the normalized angular displacement  $\theta/\alpha$  (equation 13) vs. dimensionless time  $t/\tau$  for  $\omega/p = 4$  and  $\eta = 0.95$ . The ground acceleration and the angular velocity of the block are also given on the same plot.

just before impact ( $\theta_1(t_i) = 0$ ). Substituting in equation (6) and rearranging terms gives

$$\tan \psi = \frac{\sin \omega t_i - (\omega/p) \sinh p t_i}{1 + (\omega/p)^2 - (\omega/p)^2 \cosh p t_i - \cos \omega t_i}. \quad (17)$$

Therefore, for a given  $\omega/p$ , the intersection (16) and (17) will specify  $\psi$ , which in turn determines the amplitude  $A$ .

**CASE 2:  $t_i > \tau$ .** For high-frequency ground accelerations for which the impact occurs at  $t > \tau$ , again, we divide the interval from the time that the rocking motion begins ( $t = 0$ ) to the time that the block overturns ( $t > t_i$ ) into three time windows: (a)  $0 \leq t \leq \tau$ , (b)  $\tau < t \leq t_i$ , and (c)  $t > t_i$  and solve the corresponding differential equations.

(a) The differential equation of motion and the initial conditions for the interval  $0 \leq t \leq \tau$  are identical to those of case 1 (a). Therefore, the solution is given by equation (6).

(b) For the interval  $\tau < t \leq t_i$  the inertial force is zero, and the equation of motion is

$$\ddot{\theta}_2 - p^2(\theta_2 - \alpha) = 0. \quad (18)$$

The solution to this equation subject to the following initial conditions at  $t = \tau$ ,

$$\theta_2(\tau^+) = \theta_1(\tau^-)$$

$$\dot{\theta}_2(\tau^+) = \dot{\theta}_1(\tau^+),$$

is

$$\theta_2 = \alpha + \frac{\alpha}{1 + \left(\frac{\omega}{p}\right)^2} \left[ - \left(\frac{\omega}{p}\right)^2 \cosh pt + \frac{\omega \sinh pt}{p \tan \psi} - \frac{\omega \sinh p(t - \tau)}{p \sin \psi} \right]. \quad (19)$$

(c) And after impact,  $t \geq t_i$ , the block continues its free rocking motion (no inertial force) about  $O_2$ . The solution to the equation of motion

$$\ddot{\theta}_3 - p^2(\theta_3 - \alpha) = 0 \quad (20)$$

subject to the initial conditions

$$\begin{aligned} \theta_3(t_i^+) &= \eta\theta_2(t_i^-) \\ \dot{\theta}_3(t_i^+) &= -\eta\dot{\theta}_2(t_i^-) \end{aligned}$$

is

$$\begin{aligned} \theta_3 &= \alpha - \alpha(1 - \eta) \cosh p(t - t_i) - \frac{\alpha}{1 + \left(\frac{\omega}{p}\right)^2} \\ &\left[ \eta \left(\frac{\omega}{p}\right)^2 \cosh p(t - 2t_i) + \eta \frac{\omega \sinh p(t - 2t_i)}{p \tan \psi} \right. \\ &\left. + \frac{\omega \sinh p(t - 2t_i + \tau)}{p \sin \psi} \right]. \quad (21) \end{aligned}$$

Combining equations (6), (19), and (21), the solution can be written as

$$\theta(t) = \theta_1(t)H(\tau - t) + \theta_2(t)H(t - \tau)H(t_i - t) + \theta_3(t)H(t - t_i) \quad (22)$$

where  $H(t)$  is the Heaviside unit step function.

Figure 5 shows a plot of the normalized angular displacement  $\theta/\alpha$  (equation 22) versus dimensionless time  $t/\tau$  for  $\omega/p = 8$  and  $\eta = 0.95$ . The minimum toppling acceleration amplitude is about  $8.64\alpha g$ ; and the impact occurs at  $t = 2.06\tau$ . The ground acceleration and the angular velocity of the block are also given on the same plot.

*Minimum Overturning Amplitude.* In this case, the minimum overturning condition requires that  $\dot{\theta}_3 = 0$  at  $\theta_3 = \alpha$ ; that is, the rocking block at the time of overturning must have nearly zero angular velocity. Using the conservation of total energy, the condition  $\dot{\theta}_3 = 0$  at  $\theta_3 = \alpha$  is satisfied if

$$\frac{1}{2} I \dot{\theta}_3^2(t_i) = mgR (1 - \cos(\alpha)). \quad (23)$$

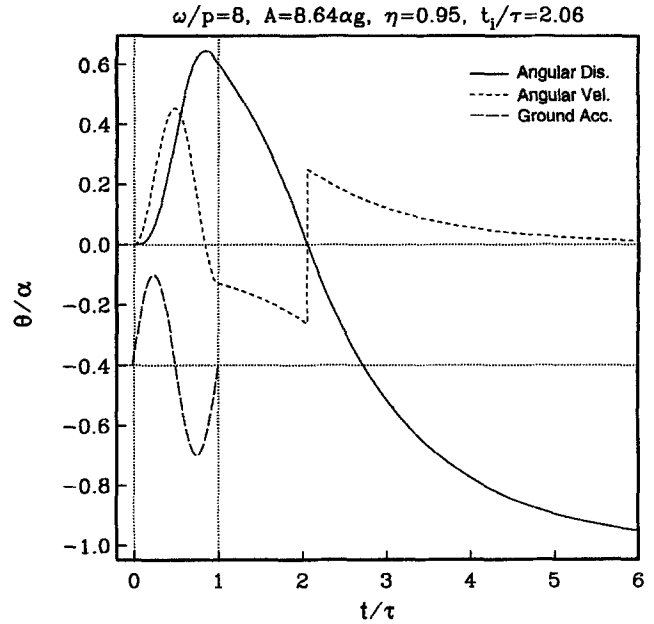


Figure 5. A plot of the normalized angular displacement  $\theta/\alpha$  (equation 22) vs. dimensionless time  $t/\tau$  for  $\omega/p = 8$  and  $\eta = 0.95$ . The ground acceleration and the angular velocity of the block are also given on the sample plot.

Again, for a small  $\alpha$ , equation (23) reduces to

$$\dot{\theta}_3(\tau) = p\alpha. \quad (24)$$

Substituting for  $\dot{\theta}_3(\tau)$  in equation (24), the overturning condition

$$\tan \psi = \frac{p/\omega}{1 - [1 + (p/\omega)^2] (1 - \eta^{-1})e^{pt_i}} \left[ -1 + \frac{e^{p\tau}}{\cos \psi} \right] \quad (25)$$

is obtained, with  $t_i$  defined by equation (17).

According to the foregoing analysis, equations (16) and (25), in conjunction with equation (17), can be used to determine the minimum amplitude  $A$  of a full sine wave that overturns a rectangular block, depending on whether  $t_i < \tau$  or  $t_i > \tau$ , respectively. The transition from  $t_i < \tau$  to  $t_i > \tau$  depends on the values of  $\omega/p$  and  $\eta$ . As shown in Figure 6, the  $A/\alpha g - \omega/p$  space can be divided into two regions, one for  $t_i < \tau$  and another for  $t_i > \tau$ . The boundary between the two regions (the solid curve) is determined by substituting  $\tau$  for  $t_i$  in equation (17), and it is independent of the coefficient of restitution  $\eta$ . The two dashed curves are plots of  $A/\alpha g$  (the minimum overturning acceleration amplitude) versus  $\omega/p$  for  $\eta = 1$  and  $\eta = 0.9$ . For  $\eta = 1$  the transition

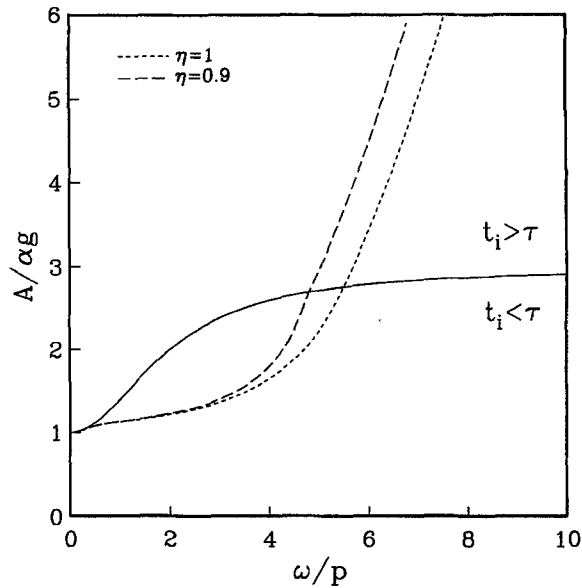


Figure 6. The solid line divides the  $A/\alpha g-\omega/p$  space into two regions, one for  $t_i < \tau$ , and another for  $t_i > \tau$ . The two dashed curves are plots of the minimum overturning acceleration amplitudes for  $\eta = 1$  (no damping) and  $\eta = 0.95$  (3% damping).

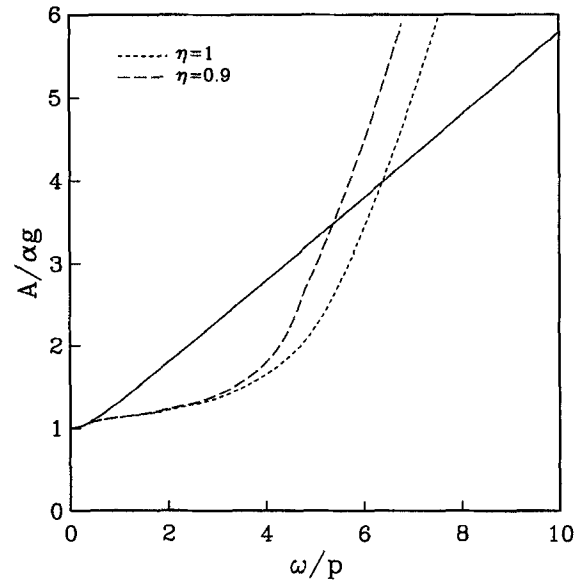


Figure 7. Plots of the normalized minimum toppling amplitude,  $A/\alpha g$ , of a full-sine-wave ground acceleration as a function of  $\omega/p$  (dashed lines). For comparison, the results for a half-sine-wave acceleration pulse is also plotted (Shi *et al.*, 1996). In the absence of damping ( $\eta = 1$ ), the half-sine-wave and full-sine-wave curves intersect at  $\omega/p = 2\pi$ .

from  $t_i < \tau$  to  $t_i > \tau$  occurs at  $\omega/p = 5.5$ ; for  $\eta = 0.9$  the transition takes place at  $\omega/p = 4.7$ .

Figure 7 shows plots of normalized minimum toppling amplitude ( $A/\alpha g$ ) of sinusoidal ground accelerations as a function of  $\omega/p$  for  $\eta = 1$  and  $\eta = 0.9$ . For comparison, the results for a half-sine-wave acceleration pulse is also plotted (Shi *et al.*, 1996). In the absence of damping ( $\eta = 1$ ), the half-sine-wave and full-sine-wave curves intersect at  $\omega/p \approx 2\pi$ . This shows that for acceleration frequencies  $f$  less than  $p$ , a full sine wave of acceleration is more efficient in overturning a rigid block than a half-sine-wave pulse; whereas for frequencies greater than  $p$  the opposite is true. For realistic situations when damping is not zero, the two curves intersect at  $\omega/p < 2\pi$ .

### Discussion and Conclusions

The locomotive of the overturned train was the narrow-gauge engine number 14, built in 1891 by Brooks and scrapped in 1935. The engine was last operated on 19 September 1926 (Dickinson *et al.*, 1967). Based on the manufacturer's specifications, we roughly estimate that  $\alpha = 0.25$  and  $p = 2.15$  Hz; and using equation (10) we estimate  $\eta$  to be about 0.9, which corresponds to a damping ratio of about 3%. Using these constants, we estimate the minimum amplitude of a full sine wave of ground acceleration,  $A$ , that would topple the locomotive, as a function of frequency,  $f$ . As shown in Figure 8, it takes an amplitude of less than 1g to topple the train at frequencies below 2 Hz.

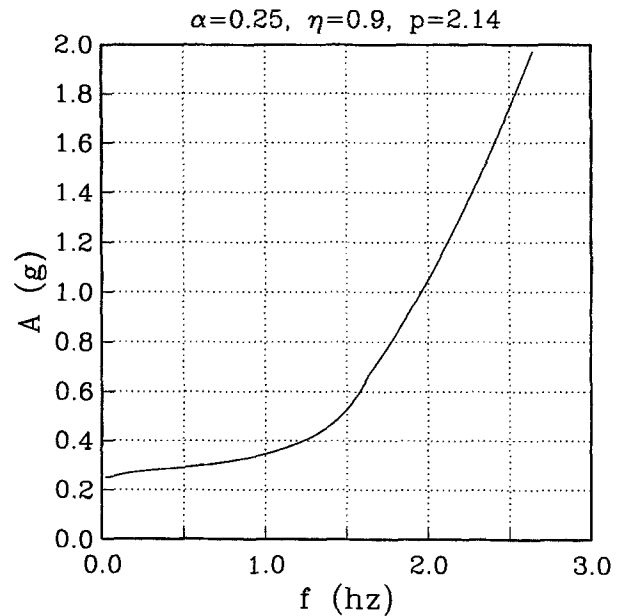


Figure 8. Toppling amplitude of a full-sine-wave ground acceleration calculated for the narrow-gauge train at Point Reyes station as a function of frequency. We have assumed that  $\alpha = 0.25$ ,  $\eta = 0.95$ , and  $p = 2.14$ .

However, since the fault-normal component of ground accelerations during an earthquake is more complicated than a full sine wave, we used a numerical technique (Shi *et al.*, 1996) to examine the response of the train to the following:

1. The synthetic data at Point Reyes Station (about 800 m northeast of the San Andreas fault) that was generated for a magnitude 8 earthquake rupturing northwest, with the epicenter about 40 km to the southeast near the Golden Gate (J. G. Anderson, personal communication)
2. The ground acceleration recordings at the Lucerne station during the 1992 Landers earthquake

In order to estimate the *minimum* peak ground acceleration (PGA), similar in shape to the Landers record or the synthetic data, that would topple the train, we multiply the input motion by a constant,  $\mu$ . This constant would be larger than unity if the original input motion ( $\mu = 1$ ) could not topple the train, and smaller than unity otherwise.

Figure 9 shows the rocking response of the narrow-gauge train to scaled accelerograms similar in shape to that of the fault-normal component of the synthetic data with a peak acceleration of about 2.5g. For  $\mu = 1$ , the train overturns with the arrival of the first pulse with an amplitude of about 1.3g. The train swings in a direction opposite to that of the ground acceleration and topples. As the value of  $\mu$  is reduced, the first pulse is no longer capable of toppling the train. For  $\mu = 0.7$  (PGA = 1.75g), the narrow-gauge train swings to one direction and then changes course and swings in the opposite direction before overturning. (This rocking response is similar to the motion experienced by the train's conductor.) For  $\mu < 0.7$ , the rocking and overturning response becomes more complex. For  $\mu$  values less than 0.45, the train rocks back and forth without toppling. Therefore, in order to topple the train, the peak ground acceleration should exceed 1.13g ( $\mu = 0.45$ ).

We also examined the response of the train to the fault-normal component of the synthetic data that had been low-pass filtered below 3 Hz. Our purpose was to study the effect of high-frequency acceleration pulses on the rocking response of the train. The result is shown in Figure 10. Again, we varied the overall amplitude of the input motion by changing the  $\mu$  value. The train began to topple when  $\mu$  exceeded about 0.4. The similarity in  $\mu$  values for the unfiltered and filtered input motions that just topple the train might suggest that the high-frequency acceleration pulses do not play a significant role. However, as we see in the next paragraph, this might be just a coincidence. The problem of rocking rigid bodies is extremely nonlinear; during the course of rocking, the arrival of each new acceleration pulse can significantly affect the motion. (Although, for a small  $\alpha$ , the equation of motion about either of the two rocking points can be linearized, the overall problem of rocking motion is nonlinear because (1) rocking will not start as long as the ground acceleration is less than  $\alpha g$ , and (2) the restoring torque changes sign at the time of impact.)

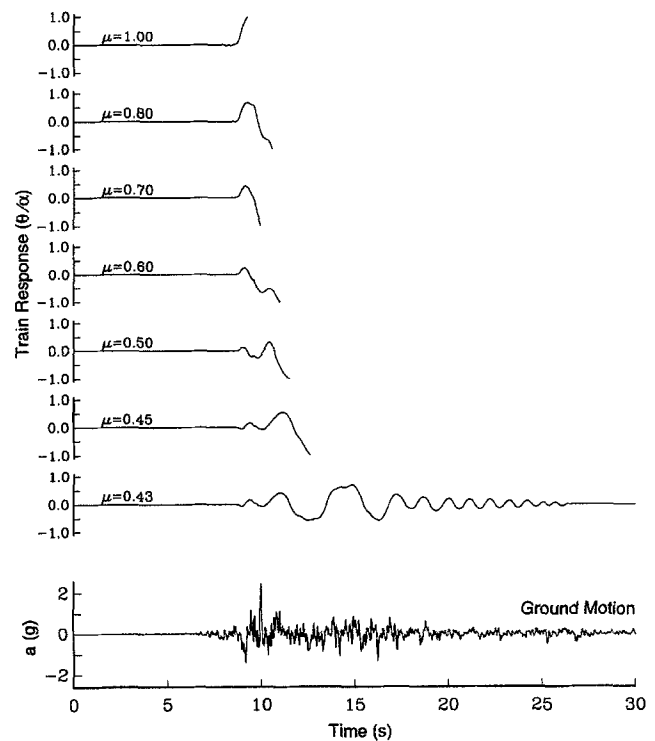


Figure 9. The rocking response of the narrow-gauge train to the scaled accelerograms similar in shape to that of the fault-normal component of the synthetic data with a peak acceleration of about 2.5g.

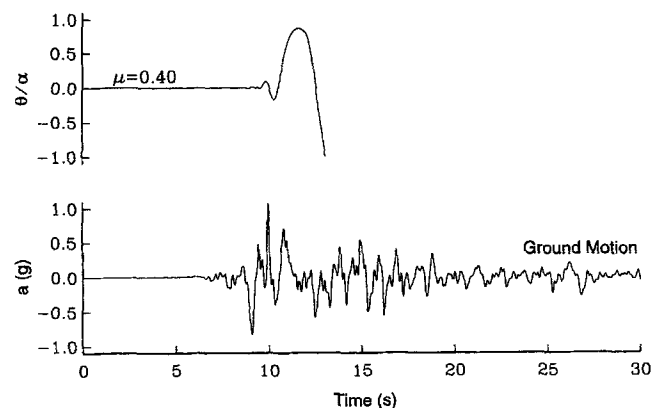


Figure 10. The rocking response of the narrow-gauge train to the scaled accelerograms similar in shape to that of the low-pass filtered fault-normal component of the synthetic data. The cutoff frequency is at 3 Hz.

Finally, we examined the response of the train to the scaled fault-normal component of the Landers accelerogram at Lucerne station (PGA = 0.71 g). For  $\mu = 1$ , although the train began to rock, it did not overturn. As we increased the value of  $\mu$ , the rocking amplitude increased too. The train started to topple when  $\mu$  exceeded 1.07 (Fig. 11). Therefore, an accelerogram, similar in shape to that of the fault-normal

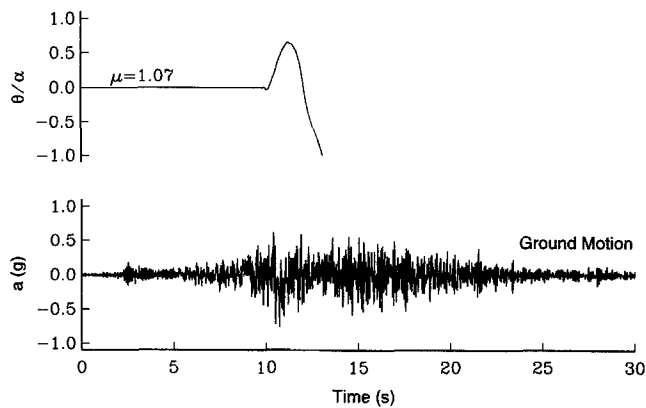


Figure 11. The rocking response of the narrow-gauge train to the scaled accelerograms similar in shape to that of the fault-normal component of the Lucerne record of the 1992 Landers earthquake.

component of Landers earthquake at Lucerne, but with a minimum peak acceleration of  $0.76g$ , would topple the narrow gauge train.

We also examined the train response to the low-pass filtered (with a cutoff frequency at 3 Hz) accelerogram at Lucerne. The filtered accelerogram, unlike the case with the synthetic data, hardly initiated the rocking motion because the ground accelerations barely exceeded the threshold rocking acceleration of  $0.25g$ . This illustrates the significant role that high-frequency acceleration pulses play in controlling the rocking motion. Although they might not be able to topple, they initiate the rocking motion if their peak value exceeds  $\alpha g$ . Once started, the rocking can be sustained with subsequent, low-amplitude, low-frequency pulses.

In summary, the analytical solution provides a lower-bound estimate of the peak ground acceleration at Point Reyes Station, assuming a full-sine-wave shape for the fault-normal component of ground accelerations. Our results indicate that for a 3% damping ratio, the minimum toppling accelerations at 1, 1.5, and 2 Hz are  $0.35g$ ,  $0.5g$ , and  $1.05g$ , respectively. For more realistic accelerograms the toppling acceleration estimates are about  $1.1g$  (complex synthetic) and  $0.76g$  (Lucerne record of the 1992 Landers earthquake).

### Acknowledgments

We would like to express our thanks to Mr. Kyle K. Wyatt, Curator of History, at the Nevada State Railroad Museum for providing us with valuable information about the overturned train. We would like to thank

John Anderson for generating the synthetic data. We are also grateful to Yuehua Zeng for his valuable comments.

### References

- Archuleta, R. J., and S. H. Seale (1995). Deterministic modeling of a San Andreas earthquake, in *Proceedings: Modeling Earthquake Ground Motions at Close Distances, Sept. 1990*, Stanford, California, J. F. Schneider and P. G. Somerville (Editors), Electric Power Research Institute Research Project 3102-04.
- Bolt, B. A. (1968). The focus of the 1906 California earthquake, *Bull. Seism. Soc. Am.* **58**, 457–471.
- Boore, D. M. (1977). Strong motion recordings of the California earthquake of April 18, 1906, *Bull. Seism. Soc. Am.* **67**, 561–577.
- Dickenson, A. B., R. Graves, T. Wurm, and A. Graves (1967). *Narrow Gauge to the Redwoods*, Trans-Anglo Books, Glendale, California.
- Hall, J. F., T. H. Heaton, M. W. Halling, and D. J. Wald (1995). Near-source ground motion and its effects on flexible buildings, *Earthquake Spectra* **11**, 569–605.
- Hartzell, S. H., and T. H. Heaton (1995). San Andreas deterministic fault problem Green's function summation for a finite source, in *Proceedings: Modeling Earthquake Ground Motions at Close Distances, September 1990*, Stanford, California, J. F. Schneider and P. G. Somerville (Editors), Electric Power Research Institute Research Project 3102-04.
- Haskell, N. A. (1969). Elastic displacements in the near-field of a propagating fault, *Bull. Seism. Soc. Am.* **59**, 865–908.
- Housner, G. W. (1963). The behavior of inverted pendulum structures during earthquakes, *Bull. Seism. Soc. Am.* **53**, 403–417.
- Iwan, W. D., and X. D. Chen (1994). Important near-field ground motion data from the Landers earthquake, in *Proceedings of the 10th European Conference on Earthquake Engineering*, Vienna, Austria, August 28–September 2, 1994.
- Jordan, D. S. (1907). The earthquake rift of 1906, in *The California Earthquake of 1906*, D. S. Jordan (Editor), A. M. Robertson (Publisher), San Francisco.
- Shi, Baoping, A. Anoshehpour, Y. Zeng, and J. N. Brune (1996). Rocking and overturning of precariously balanced rocks by earthquakes, *Bull. Seism. Soc. Am.* **86**, 1364–1371.
- Wald, D. J., and T. H. Heaton (1994). Spatial and temporal distribution of slip for the 1992 Landers, California, earthquake, *Bull. Seism. Soc. Am.* **84**, 668–691.

University of Nevada, Reno  
Seismological Laboratory 174  
Mackay School of Mines  
Reno, Nevada 89557-0141  
(A.A., B.S., J.N.B.)

California Institute of Technology  
Dept. of Civil Engineering, MS 104-44  
Pasadena, CA 91125  
(T.H.H.)

Manuscript received 7 December 1998.